Multi-classification of Cell Deformation Based on Object Alignment and Run Length Statistic

Heng Li, *Student Member*, *IEEE*, Zhiwen Liu, *Member*, *IEEE*, Xing An, and Yonggang Shi

***Abstract*—Cellular morphology is widely applied in digital pathology and is essential for improving our understanding of the basic physiological processes of organisms. One of the main issues of application is to develop efficient methods for cell deformation measurement. We propose an innovative indirect approach to analyze dynamic cell morphology in image sequences. The proposed approach considers both the cellular shape change and cytoplasm variation, and takes each frame in the image sequence into account. The cell deformation is measured by the minimum energy function of object alignment, which is invariant to object pose. Then an indirect analysis strategy is employed to overcome the limitation of gradual deformation by run length statistic. We demonstrate the power of the proposed approach with one application: multi-classification of cell deformation. Experimental results show that the proposed method is sensitive to the morphology variation and performs better than standard shape representation methods.**

I. INTRODUCTION

Cellular morphology, including cellular shape and cytoplasmic distribution, is a kind of large-scale expression of the global organizational and physiological state of cells. It is resulted from the complex interactions involving the cytoskeleton, the membrane and membrane-bound proteins, and the extracellular environment [1]. Cell deformation, namely cellular morphology variation, takes place during multiple physiological processes, such as wound healing, the immune response and cancer metastasis [2]. According to this, cell morphology has become a standard theory for computerized cell image processing and pattern recognition [3] [4].

The analysis on static cellular images, such as cell segmentation, cell shape representation, is widely applied to observe and investigate cellular physiological activity. However, static images cannot provide information about the dynamic activity. As a consequence, more and more attention has been paid to live-cell (2D+t) imaging, since it can provide more information about cell morphology change, and a greater insight into the nature of cellular functions [2]. To apply dynamic cell morphology in practice, computational tools are increasingly necessary in order to extract information from vast quantities of data.

Live-cell is a non-rigid body, and it deforms arbitrarily, subtly and gradually. While the traditional shape descriptors are efficiently for representing rigid global shape. It is complex to apply the shape descriptors to analyze live-cell deformation, since their invariance of pose elements (translation, rotation and scale) is limited [5]. And shape descriptors disregard the alteration of gray value, in other words, the cytoplasm variation is ignored. In addition, the cell deformation in successive frames is too tiny for shape descriptors to measure.

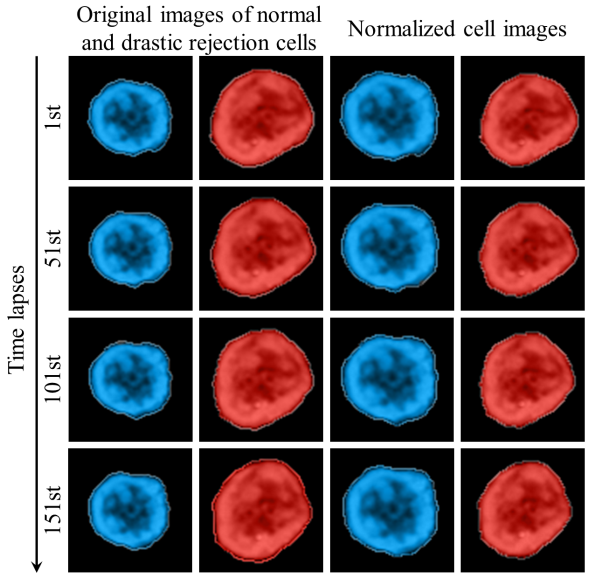

Fig. 1. Results of sequence scale normalization; first two columns are the original frames of two videos, the following two are the zoomed frames. The rows are the 1st, 51st, 101st and 151st frames of the image sequences.

In this paper, we present an innovative approach to describe the cell deformation by the minimum energy function of object alignment, which captures image dissimilarity without the influence of object pose, and takes full use of the shape change and the cytoplasm variation. Besides, an indirect strategy using run length statistic is introduced to overcome the problem of tiny deformation, and consider the entire frames in a video. The results of our experiment show that the proposed method makes a significant improvement in multi-classification of cell deformation.

II. METHODS

A. Scale normalization in sequences

Cells have diverse size, so it is essential to eliminate the influence of scale during the analysis of cell deformation. To achieve scale invariance, the conventional shape represent methods normalize the descriptors by eliminating the information of size [5]. This procedure is suitable to static image analysis. Nevertheless, cell deformation is also accompanied

*This work is supported by the National Natural Science Foundation of China (61271112)

The authors are with School of Information and Electronics, Beijing Institute of Technology, Beijing, China. (email: heng.li@bit.edu.cn, zwliu@bit.edu.cn, anxing512@126.com, ygshi@bit.edu.cn).

978-1-4244-7929-0/14/$26.00 ©2014 IEEE

with cellular size change. There is no wonder that the information of deformation in image sequence is deserted with the size normalization framework of shape representation.

For the application of image sequence, our analysis approach begins with sequence scale normalization. The sequence scale normalization deems the cell size in the first frame of each video as an original parameter. The size scale of a video is captured from the ratio of the average of original cellular area in all frames and the corresponding original parameter. The frames in the identical video are zoomed by the size scale of the video (Fig.1). In this way, the influence of cell scale is eliminated; meanwhile the information of deformation is preserved. The sequence scale normalization is given by

$$a'_{in} = \frac{\overline{A}}{a_{i1}} a_{in} \tag{1}$$

where a_{in} is the crude cell size, and a'_{in} is the regularized cell size, $\overline{A}$ represents the average of the original parameters. n and i refer to the numerical order of the videos and the frames respectively.

B. Object alignment

Cell deformation consists of shape change and cytoplasm variation. Therefore it is hard to guarantee the homogeneity of shape change and cytoplasm variation. Object alignment aims to recover a global transformation, such as rigid, similarity, or affine transformation, that brings the pose of a source object as close as possible to that of a target object. The most notable characteristics of object alignment are its global concern and robustness to object pose. This inspires us to introduce object alignment into cell deformation analysis.

Energy function is constantly employed by object alignment methods, which achieve alignment by minimizing the energy function. The main idea of our method is to use the minimized energy function to reveal the morphology change. We modify an efficient region object alignment method to cope with gray-scale image, and introduce the energy function to measure the cell deformation [6]. As the scale is already normalized, let pose parameter $\mathrm{P} = \begin{bmatrix} a & b & \theta \end{bmatrix}^{\mathrm{T}}$ with a , b , θ corresponding to x , y-translation, and rotation, respectively. The transformation of image is defined as

$$\widetilde{I}(\widetilde{x}, \widetilde{y}) = \mathrm{T}[I(x, y)] \tag{2}$$

where

$$\begin{bmatrix} \widetilde{x} \\ \widetilde{y} \\ 1 \end{bmatrix} = \mathrm{T}[\mathrm{P}] \begin{bmatrix} x \\ y \\ 1 \end{bmatrix} = \begin{bmatrix} 1 & 0 & a \\ 0 & 1 & b \\ 0 & 0 & 1 \end{bmatrix} \times \begin{bmatrix} \cos(\theta) & -\sin(\theta) & 0 \\ \sin(\theta) & \cos(\theta) & 0 \\ 0 & 0 & 1 \end{bmatrix} \begin{bmatrix} x \\ y \\ 1 \end{bmatrix} \tag{3}$$

$I(x, y)$ and $\widetilde{I}(\widetilde{x}, \widetilde{y})$ represent original image and transformed image respectively. The transformation matrix $\mathrm{T}[\mathrm{P}]$ maps the coordinates (x, y) into coordinates $(\widetilde{x}, \widetilde{y})$.

The source image and target image are aligned by using gradient descent to minimize the following energy function:

$$E = \frac{\iint_{\Omega} \left(\widetilde{I}_s - I_t\right)^2 \mathrm{d}A}{\iint_{\Omega} \left(\widetilde{I}_s + I_t\right)^2 \mathrm{d}A} \tag{4}$$

where Ω denotes the image domain. I_t is the target image, and $\widetilde{I}_s$ is the transformed source image.

The gradient of E taken with respect to P is given by

$$\nabla_{\mathrm{P}} E = \frac{2 \iint_{\Omega} \left(\widetilde{I}_s - I_t\right) \nabla_{\mathrm{P}} \widetilde{I}_s \mathrm{d}A}{\iint_{\Omega} \left(\widetilde{I}_s + I_t\right)^2 \mathrm{d}A} - \frac{2 \iint_{\Omega} \left(\widetilde{I}_s - I_t\right)^2 \mathrm{d}A \iint_{\Omega} \left(\widetilde{I}_s + I_t\right) \nabla_{\mathrm{P}} \widetilde{I}_s \mathrm{d}A}{\left(\iint_{\Omega} \left(\widetilde{I}_s + I_t\right)^2 \mathrm{d}A\right)^2} \tag{5}$$

where $\nabla_{\mathrm{P}} \widetilde{I}_s$ refers to the gradient of the transformed image taken $\widetilde{I}_s$ with respect to the pose parameter P.

We treat two cell images as the source and the target object respectively. The pose of the source cell is brought closest to the target cell, when E achieves its minimum. By now, E reveals the global difference between the two cells, without the influence from the object pose. Thus $E_{\min}$, which is defined as the minimum of E, is used as the value of the dissimilarity between cells.

C. Run Length Statistic

Because the live-cell morphology deforms arbitrarily, subtly and gradually, it has limitations on measuring the deformation between successive frames. The conventional analysis strategy is to interval sample the image sequences [7]. Nevertheless, this framework greatly reduces the data volume, for only a few frames of the video are used. Besides, the information of deformation in the interval is dumped. To address this problem, we presented a modified strategy. Run length statistic

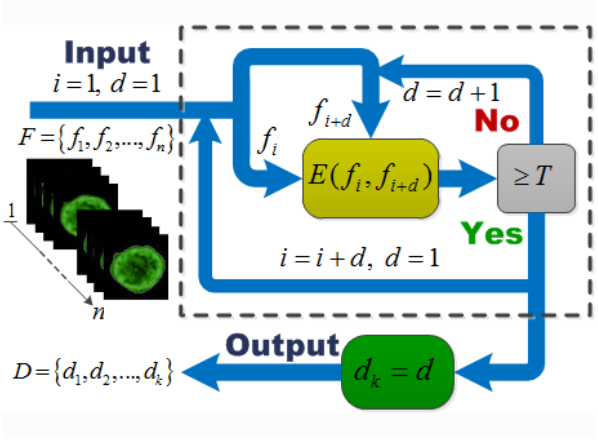

Fig. 2. Flowchart of Run Length Statistic

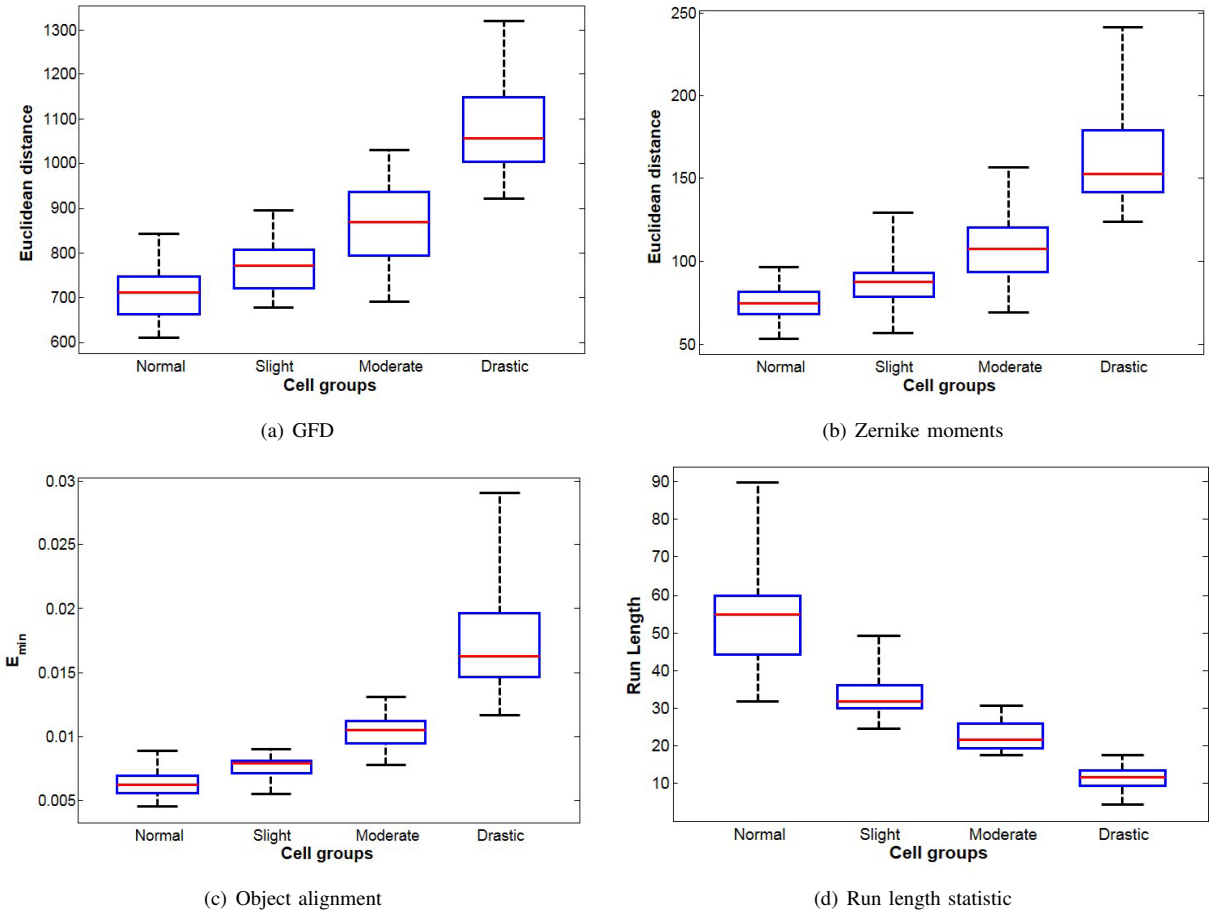

(a) GFD

(b) Zernike moments

(c) Object alignment

(d) Run length statistic

Fig. 3. Results of different methods; (a) (b) are the mean Euclidean distance of GFD and Zernike moments, (c) (d) are the mean $E_{\min}$ and run length of object alignment. In contrary to other results, the higher rejection cells have shorter run length. The videos are arranged in descending according to their values.

is applied to take the full use of all frames by indirectly comparing their differences.

The modified strategy begins with the conventional method, a sequence of dissimilarity is captured by interval sample. To minimize the impact of outliers, the dissimilarity sequence is represented by its median. Then the average of the medians of the entire videos is used as a threshold, which is defined as

$$T = \frac{\sum \text{median}\,[\mathrm{E}_i]}{N} \tag{6}$$

where E_i represents the dissimilarity sequence of the videos, N is the total number of the videos.

Then the first frame is regard as an initial target frame. The source frame is the following frame, which is closest to the target one and satisfies $E_{\min}$ of target and source frame not less than the threshold. The run length between target and source frame is recorded as the value of their dissimilarity. Then the former source frame is employed as the new target frame. The last procedure is iterated until the end of the video. Finally, the mean of this run length statistic sequence of dissimilarity is regarded as the measurement of cell deformation of the corresponding video. It is given by

$$L = \overline{\mathrm{D}} \tag{7}$$

where

$$\mathrm{D} = \{d | E_{\min}\left(F_n, F_{n+d}\right) \geq T, \text{and } E_{\min}\left(F_n, F_{n+d-1}\right) < T\} \tag{8}$$

F_n represents the frames, d is the run length between target frame and source frame, D refers to the sequence of d.

Fig.2 illustrates the flowchart of run length statistic. L is used as the final measurement of the morphology variation. The entire frames are now taken into account to analyze the cell image sequences.

III. EXPERIMENTS AND RESULTS

A. Experimental Data

To evaluate the performances of the proposed approach, we conducted the experiment on a group of data, which consists of 100 lymphocyte video clips (20-30 seconds) taken from the cooperation hospital−−Beijing You'an Hospital. The lymphocytes were obtained from blood samples of 100 mice undergoing back skin transplantation (age: 6-8 weeks, weight:

TABLE I
MULTI-CLASSIFICATION RESULTS OF CELL SEQUENCES USING LVQ.

Method	TrPr(%)	TePr(%)	TrRe(%)	TeRe(%)	TrF(%)	TeF(%)
GFD	69.76	62.78	66.67	57.69	66.17	56.42
Zernike moments	71.95	67.33	64.58	63.46	62.25	58.34
Object alignment	82.43	78.41	79.17	76.92	76.24	73.53
Run length statistic	85.19	83.56	85.42	84.62	84.76	83.91

20-22 g) collected from the tail 7 days after the skin transplant. Clean healthy Balb/c male mice and C57BL/6 male mice are used as the hosts and the donors. The video clips were observed with phase contrast microscopy (Olympus BX51, 0.3 μm resolution) at a magnification of 16 $\times$ 1000. The video clips are divided into four sets (no rejection, slight rejection, moderate rejection and drastic rejection) by experts and relevant researchers according to the cell deformation.

B. Results and Discussion

The experiment is conducted on multi-classification of immune cells, and the proposed method is compared with generic Fourier descriptor (GFD) and Zernike moments, two of the most efficient shape descriptors [1] [5]. The performance of object alignment without run length statistic is also shown in the results. For the shape descriptors, the origin of coordinates is set at the centroid of the object to get shift invariance. Since in our application the cellular area has already been normalized, we do not normalize the coefficients of shape descriptors. The Zernike moments is calculated to 30 orders, which is sufficient to reproduce most shapes. The results of all the celluar data are demonstrated in Fig.3. Finally, Learning Vector Quantization (LVQ) was then applied to classify these four categories, where 12 cellular data of each group is utilised as train data, and the else data is test data. Table I shows the comparison results of mean recognition precision (TrPr, TePr), recall rate (TrRe, TeRe) and F-score (TrF, TeF) of training and testing for these methods.

It can be seen in Fig.3, the cells in groups of moderate rejection and drastic rejection can be more clearly identified than those in groups of normal and slight rejection by each of the methods. This is due to not only cellular shape but also cytoplasm varies immensely in the condition of intense rejection. On the other hand, the cells under slight rejection are confused with the normal cells in the results of GFD and Zernike moments. The gentle cellular shape change makes the shape descriptors powerless. Not taking the cytoplasm variation into account causes their poor performance on the classification of normal and slight rejection cells.

As a consequence of considering both the cellular shape change and the cytoplasm variation, the proposed method performs effectively on the classification of cells in the four levels. Comparing with only using object alignment, the strategy of run length statistic shows an outstanding performance. The gaps between different groups in the result of run length statistic are more conspicuous than other results. The indirect strategy using run length statistic takes full use of the entire information of cell deformation by considering each frame in the image sequence. As seen in Table I, our method makes a significant improvement of multi-classification of cells in different rejection levels. The performance of the proposed algorithm overcomes the standard shape representation methods in precision, recall rate and F-score.

IV. CONCLUSIONS

In this paper, we have proposed a novel and efficient approach for cell deformation measurement. Such an approach is applied by aligning frames in cell image sequences, and the indirect analysis of the dissimilarity between successive frames. It measures cell deformation accurately by taking the cell shape change and the cytoplasm variation into account. Meanwhile it takes full use of each frame in the image sequence. The invariance to object pose also enables the method a satisfying performance. Compared with standard shape representation methods, our algorithm performs much better on multi-classification of the cellular morphology variation in different rejection levels, and can provide more information of the global organizational and physiological state of cells.

ACKNOWLEDGMENTS

The cellular video data is provided by Beijing You'an Hospital.

REFERENCES

[1] Z. Pincus and J. Theriot, "Comparison of quantitative methods for cell-shape analysis," Journal of microscopy, vol. 227, pp. 140-156, 2007.
[2] X. An, Z. Liu, Y. Shi, N. Li, Y. Wang, and S. Joshi, "Modeling Dynamic Cellular Morphology in Images," in Medical Image Computing and Computer-Assisted Intervention−MICCAI 2012, 2012, pp. 340-347.
[3] S. Chen, M. Zhao, G. Wu, C. Yao, and J. Zhang, "Recent advances in morphological cell image analysis," Computational and mathematical methods in medicine, vol. 2012, 2012.
[4] V. Nandakumar, L. Kelbauskas, R. Johnson, and D. Meldrum, "Quantitative characterization of preneoplastic progression using single-cell computed tomography and three-dimensional karyometry," Cytometry Part A, vol. 79, pp. 25-34, 2011.
[5] C. Singh, and P. Sharma, "Performance analysis of various local and global shape descriptors for image retrieval," Multimedia systems, vol.19, pp. 339-357, 2013.
[6] A. Tsai, A. Yezzi Jr, W. Wells, C. Tempany, D. Tucker, A. Fan, et al., "A shape-based approach to the segmentation of medical imagery using level sets," Medical Imaging, IEEE Transactions on, vol. 22, pp. 137-154 2003.
[7] Y. Huang, Z. Liu, Y. Shi, N. Li, X. An, and X. Gou, "Quantitative Analysis of Lymphocytes Morphology and Motion in Intravital Microscopic Images," in Engineering in Medicine and Biology Society (EMBC), 2013 35th Annual International Conference of the IEEE, 2013, pp. 3686-3689.